

Carbon Nanotube-Hybridized Supramolecular Hydrogel Based on PEO-*b*-PPO-*b*-PEO/ α -Cyclodextrin as a Potential Biomaterial

Zhongying Hui,^{1,2} Xiaolan Zhang,¹ Jiahui Yu,² Jin Huang,^{1,2} Zhongshi Liang,² Daxin Wang,³ Haitao Huang,¹ Peihu Xu¹

¹College of Chemical Engineering and Affiliated Hospital, Wuhan University of Technology, Wuhan 430070, China

²Institutes for Advanced Interdisciplinary Research, East China Normal University, Shanghai 200062, China

³Subei Hospital of Jiangsu Province, Yangzhou University, Yangzhou 225001, China

Received 18 July 2009; accepted 4 November 2009

DOI 10.1002/app.31729

Published online 5 January 2010 in Wiley InterScience (www.interscience.wiley.com).

ABSTRACT: In virtue of the potential biomedical application of carbon nanotube (CNT), the CNT was hybridized into a supramolecular hydrogel based on the selective inclusion of α -cyclodextrin (α -CD) onto poly(ethylene oxide) (PEO) segments of a triblock copolymer, i.e., PEO-*block*-poly(propylene oxide)-*block*-PEO. Different from the previous report, the content of α -CD, in contrast to that of ethylene oxide unit, was decreased to decrease the network density in hydrogel and hence improve the diffusion of encapsulated substances. As a result, the modulus of the hydrogels climbed slightly after introducing CNT. Furthermore, as the essential properties for wound dressing, the antimicrobial activity, the skin-adhesion, and water-

retention of such supramolecular hybrid hydrogels were also verified. On the other hand, the supramolecular hybrid hydrogels inherited the shear-thinning property and are suitable as an injectable biomaterial. The cell viability assay confirmed the equivalent cytotoxicity of the supramolecular hybrid hydrogels to that of the native hydrogels without CNT. Consequently, such CNT-hybridized supramolecular hydrogel shows a great potential in the biomedical application. © 2010 Wiley Periodicals, Inc. *J Appl Polym Sci* 116: 1894–1901, 2010

Key words: supramolecular hydrogel; carbon nanotube; hybrid; biomaterial

INTRODUCTION

As is well known, cyclodextrin (CD) can thread the polymer chains to produce a rod-like supramolecular polymer named as polyrotaxane (PR).^{1–3} The spontaneous aggregation of PRs plays a role of physical crosslinking for inducing the formation of supra-

molecular hydrogel,^{4–19} which is one of the most promising biomaterials based on the CD/polymer inclusion. Such physical hydrogels possessed a reversible sol-gel transition functioned as temperature^{4–9} and shearing,^{10–12} due to the dynamic characters of the host-guest recognition and noncovalent aggregation. As a result, the unique stimulus-response property of this supramolecular hydrogel has sparked great interest as an injectable biomaterial, such as the sustained-release system of drug^{10,12–14} and the scaffold of tissue engineering,^{10,12} owing to their biocompatible components. In this case, the higher molecular weight poly(ethylene oxide) (PEO) could be included by α -CD to produce a hydrogel, instead of traditional crystalline precipitate, on account of the presence of uncovered hydrophilic PEO segment.¹⁰ Furthermore, block copolymers were also used to fabricate the hydrogels induced by the CD inclusion.^{7,8,11–14} Except that the aggregation of CD-based PRs played a physical-crosslinked point, the uncovered hydrophobic segments also tended to aggregate, and hence facilitated the formation of hydrogel and enhanced the strength of the hydrogel.⁷ In addition, the uncovered ionic segment contributed to the pH-dependence of the hydrogel formation and the pH-sensitivity of gel-sol

Correspondence to: J. Huang (huangjin@iccas.ac.cn) or D. Wang (daxinw@sina.com).

Contract grant sponsor: The 973 Projects of Chinese Ministry of Science and Technology; contract grant numbers: 2007CB936104, 2009CB930300.

Contract grant sponsor: National Natural Science Foundation of China; contract grant numbers: 20404014, 20504010.

Contract grant sponsor: Shanghai Municipality Commission for Special Project of Nanometer Science and Technology; contract grant numbers: 0752nm022, 0852nm03700, 0952nm05300.

Contract grant sponsor: Shanghai Municipality Commission for Non-governmental International Corporation Project; contract grant number: 09540709000.

Contract grant sponsor: Youth Chenguang Program of Science & Technology in Wuhan; contract grant number: 200850731383.

Journal of Applied Polymer Science, Vol. 116, 1894–1901 (2010)
© 2010 Wiley Periodicals, Inc.

TABLE I
BRR and Diameters of Inhibition Zone of Hydrogels in *Escherichia coli* and *Staphylococcus aureus*, Respectively

Sample code	<i>Escherichia coli</i>			<i>Staphylococcus aureus</i>		
	d_0 (mm)	D_0 (mm)	BRR (%)	d_0 (mm)	D_0 (mm)	BRR (%)
EPE/CD	0.9	1.2	44.4	0.9	1.2	33.3
EPE/CD/CNT	0.7	1.2	71.4	0.7	1.0	42.9

transition.^{4,11} Born out of growing interest in the predominant properties attributed to nanoparticles in nanocomposites, some work concerning supramolecular hybrid and nanocomposite hydrogels based on the CD/polymer inclusion have been developed.^{9,20–22} The incorporated nanoparticles not only accelerated the formation of hydrogel²⁰ but also regulated the mechanical properties of the hydrogel.²¹ Especially, the function of the nanoparticles might be in favor of extending the application of supramolecular hydrogels.^{9,20–22}

With a rapid development of carbon nanotube (CNT) in the field of nanocomposite materials, the nanosecurity and biomedical application of CNT have also attracted much attention.²³ Based on various covalent and noncovalent modification methodologies for improving function and solubility of CNTs, many bioapplication opportunities have been created, such as biosensors,²⁴ drug and other delivery systems,^{25–27} and bioimaging.²⁸ In addition, except for the attractive structural reinforcement of CNT,^{29–31} the CNTs could impart novel properties into bioscaffolds, such as electrical conductivity. As reported, the electrical conductivity could aid to directing cell growth.^{32,33} However, the biocompatibility and bioavailability of CNTs are still discussed and verified because it is essential for the currently pursued bioapplications,^{34,35} which certainly will meet the challenge of nanosecurity.

In previous report,²⁰ the supramolecular hydrogels based on the selectively inclusion of CD onto PEO-*block*-poly(propylene oxide)-*block*-PEO have been hybridized with single-walled CNT (SWCNT). This kind of hybridized hydrogel inherited shear-thinning property, and hence showed a promising application as an injectable biomaterial. Especially, the shear-thinning property of such supramolecular hydrogel could contribute to the flowability in the sol form for the injection methodology, and then rapid become gelation *in situ* in body. In this work, except for the basic structural characterization, we further investigated the bioapplication potential of such CNT-hybridized supramolecular hydrogels and some interesting properties used for wound dressing and injectable biomaterial. By the way, the content of α -CD, in contrast to that of EO unit, was designedly decreased to decrease network density, which

might be in favor of improving diffusion of encapsulated drug or other substances.

EXPERIMENTAL

Materials

PEO₁₃₇-*b*-PPO₄₄-*b*-PEO₁₃₇ (EPE) containing 82.5 wt % PEO, with a number-average molecular weight (M_n) of 14,600, was purchased from Aldrich. α -CD was also purchased from Aldrich. CNT, with a diameter of about 10–15 nm and a purity of 90%, was kindly provided by Shenzhen Bill Tech (Shenzhen, China). RPMI 1640 cell culture medium was purchased from Gibco BRL (Paris, France). 3-[4,5-Dimethylthiazol-2-yl]-2,5-diphenyl tetrazolium bromide (MTT) and dimethyl sulfoxide (DMSO) were purchased from Sigma (St. Louis, MO).

Cell line and culture

Mouse fibroblast cell line L-929 was supplied from Institute of Biochemistry and Cell Biology, Chinese Academy of Sciences (Shanghai, China). Cells were thawed and cultured in RPMI 1640, supplemented with 10% fetal bovine serum (HyClone, Logan, Utah), streptomycin at 100 $\mu\text{g mL}^{-1}$, and penicillin at 100 U mL^{-1} . All cells were incubated at 37°C in humidified 5% CO₂ atmosphere. Cells were split by using trypsin/EDTA solution when almost confluent.

Preparation of the CNT/EPE suspensions

Four hundred milligrams of EPE and forty milligrams of CNT were placed into 20 mL of deionized water under an ultrasonic treatment, and produced a stable suspension depending upon the physical interaction between EPE and CNT. Then, the aggregated CNT agglomerates and impurities were removed by supercentrifuging at 8000 rpm for 30 min. The upper aqueous suspension was collected for the preparation of hydrogel. Meanwhile, to estimate the exact concentration of CNT and EPE in the upper aqueous suspension, we weighed the vacuum-dried precipitate, and chose a small amount of upper aqueous suspension followed by vacuum-

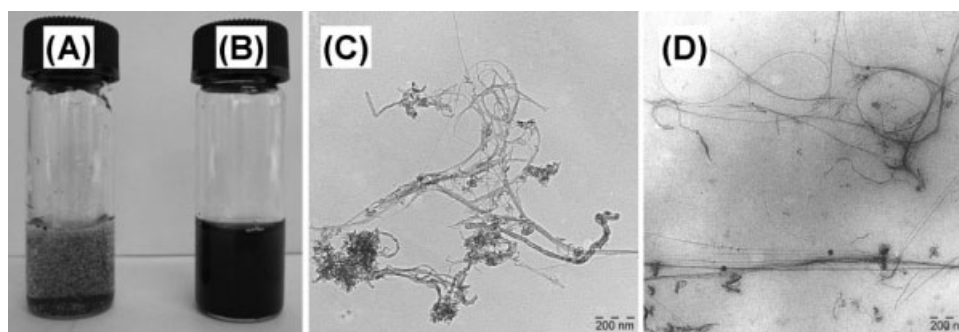


Figure 1 Visualization (A and B) and TEM images (C and D) of CNT in aqueous solutions without EPE (A and C) and in the EPE aqueous solution (B and D).

dried and measured by thermogravimetric analysis (TGA). The results showed that the weight percentage of CNT in the solid components of upper aqueous suspension, i.e., EPE and CNT, was 11.1 wt % whereas the content of CNT in the upper solution was 29.9 mg.

As reported,^{36,37} the triblock copolymer of PEO-*b*-PPO-*b*-PEO could reduce the aggregation of the exfoliation of the SWCNT and form a uniform dispersion of SWCNT in aqueous solution with the assistance of ultrasonic. In this work, the presence of EPE also resulted in a stable suspension with the uniformly dispersed CNTs [seen in Fig. 1(B)], in contrast with the aggregated CNT agglomerates in aqueous solution [Fig. 1(A)]. Meanwhile, the TEM image of Figure 1(C) shows an evident aggregation of CNT. On the contrary, the exfoliated individual CNTs can be clearly observed from the TEM image [Fig. 1(D)] due to the presence of EPE. Thus, the results of TEM image further validated that EPE could effectively improve the dispersion of CNT in aqueous solution.

Preparation of hybrid and native hydrogels

The general protocol of fabricating native EPE/CD hydrogel and hybrid EPE/CD/CNT hydrogel was described as follows: the quantitative α -CD was dissolved in water to form a transparent solution, and then mixed with the homogeneous aqueous suspension containing CNT and EPE mentioned above by a given volume ratio for α -CD solution and EPE/CNT suspension. In this mixture, the concentrations of α -CD and EPE were respectively 82.6 mg mL⁻¹ and 10.0 mg mL⁻¹, and the molar ratio of EO unit to α -CD was 2.2, which is designedly regulated as higher than a theoretical molar ratio of α -CD/PEO inclusion as 2.0 used in previous report.²⁰ Ultimately, the hybrid hydrogel containing about 0.1 wt % CNTs was prepared. In this hybrid hydrogel, the decreased content of α -CD resulted in the relatively less α -CD-based PR as the precursor of physical crosslinking, and hence gave lower network density. At the same time, the native EPE/CD hydrogel was also pre-

pared according to the earlier process when the EPE/CNT suspension was replaced by neat EPE solution.

Characterization

TGA was measured on an STA 449 C thermogravimetric analyzer (Netzsch, Germany) at a heating rate of 20°C min⁻¹ under a nitrogen atmosphere.

X-ray diffraction (XRD) measurement of the freeze-dried hydrogel powder was performed on a D/max-250 X-ray diffractometer (Rigaku Denki, Japan) equipped with a Cu K α radiation source ($\lambda = 0.154$ nm). The diffraction data were collected in a range of $2\theta = 5\text{--}60^\circ$ using a fixed time mode with a step interval of 0.02°.

The hydrogels were directly freeze-dried onto the silicon wafer for observing the morphologies by scanning electronic microscopy (SEM). SEM observation was carried out on an S-3000N scanning electron microscope (Hitachi, Japan) with an acceleration voltage of 5.0 kV after the tested samples were coated with gold.

TEM observations of the CNT aqueous suspensions with and without EPE were conducted on an H-7000FA transmission electron microscope (Hitachi, Japan) at an acceleration voltage of 75 kV. The CNT aqueous suspensions with and without EPE were spread onto Cu grids coated with carbon films followed by evaporation, respectively.

According to the reported method,³⁸ the rheological behaviors of the hydrogels were measured on an ARES-RFS III rheometer (TA Instruments) with parallel plate geometry with a diameter of 50 mm. The gap distance between two plates was fixed at 1 mm. A frequency sweep test was conducted on each sample to determine the values of storage modulus (G') and loss modulus (G'') over the frequency (ω) range from 0.1 to 100 rad s⁻¹ at 25°C. The steady flow behaviors were performed at a shear rate range from 0.01 to 50 s⁻¹. Dynamic strain sweep measurements were carried out at 1 rad s⁻¹ to determine the linear viscoelastic regime with a strain range from 0.1% to

100%. Temperature control was established by a Julabo FS 18 cooling/heating bath kept within $\pm 0.5^\circ\text{C}$ over an extended time.

Water-retention performance

The good adhesion performance of such hydrogels on scarfskin shows a potential as wound dressing. As a result, the other important property, i.e., water-retention, must be under consideration. The hydrogels as wound dressing should exhibit a low water-loss performance. In the water-retention measurement, the hydrogels with a given weight (W_0) were set in an obturator at under an ambient temperature. After the given interval, the hydrogels were weighed as W_t , and the water-loss in hydrogels against time, which is equal to the decrease of weight, was calculated according to the following equation³⁹:

$$\text{Water loss (\%)} = \frac{W_0 - W_t}{W_0} \times 100\% \quad (1)$$

Cell viability assay

Cytotoxicity was evaluated by MTT method. L929 cells were seeded in 96-well plates at an initial density of 1×10^4 cells/well in 100 μL RPMI 1640 growth medium and incubated for 18–20 h to reach 80% confluency at the time of treatment. Growth medium was replaced with 100 μL fresh media containing various amounts of EPE/CD or the hybrid EPE/CD/CNT hydrogel. Cells were incubated, and the incubation time was fixed as 24 h. And then, 10 μL of MTT solution (0.5 mg mL^{-1}) was added to the culture medium. After further incubation for 4 h in incubator, 100 μL of DMSO was added to each well to replace the culture medium and dissolve the formazan crystals. The optical density (OD) was measured at 570 nm using an automatic BIO-TEK microplate reader (Powerwave XS), and the cell viability was calculated from following equation:

$$\text{cell viability (\%)} = \frac{\text{OD}_{\text{sample}}}{\text{OD}_{\text{control}}} \times 100\% \quad (2)$$

where $\text{OD}_{\text{sample}}$ represents an OD value from a well treated with samples and $\text{OD}_{\text{control}}$ from a well treated with phosphate buffered saline (PBS) buffer only. Each experiment was carried out in triplicate. Means and corresponding standard deviations (mean \pm SD) were shown as results.

Antimicrobial activity test

The antimicrobial activities of native EPE/CD hydrogel and hybrid EPE/CD/CNT hydrogel

against *Escherichia coli* and *Staphylococcus aureus* were examined by the inhibition zone method. We adopted broth medium supplemented with 0.5% beef extract, 1% peptone, 1% NaCl, 2% agar, and 20 mL of deionized water as anaerobe medium. Sterilized medium was poured into culture dish and kept still for certain time to form a plate. Simultaneously, we prepared bacterial suspension through adding *Escherichia coli* (or *Staphylococcus aureus*) into PBS and the concentration of *Escherichia coli* (or *Staphylococcus aureus*) was fixed to be of 15–30 cfu mL^{-1} . Subsequently, we poured bacterial suspension into culture dish and placed hydrogel sample in the center of plate, which was incubated at 37°C for 24 h. After incubation, we calculated the inhibitory rate (BRR) by measuring the inside and outside diameter of inhibition zone. The BRR was calculated as follows:

$$\text{BRR (\%)} = \frac{D_0 - d_0}{d_0} \times 100\% \quad (3)$$

where D_0 and d_0 are diameters of inhibition zone and hydrogels, respectively. An average value of three replicates for each sample was taken.

RESULTS AND DISCUSSION

Formation and adhesion of hydrogels

The process of gelation is visualized in Figure 2. It was interesting to note that the CNT might accelerate the formation of supramolecular hydrogels, namely the CNT-hybridized system failed to fluidity at about 30 min whereas the native hydrogel formed until 55 min. The decrease of gelation time could be in favor of the injectable implantation.

In addition, both hybrid and native hydrogels showed a good adhesion performance on the scarfskin of human being, which is the essential property for wound dressing. Figure 3 visualizes the adhesion behavior of hydrogels onto the finger of human being. Obviously, the hydrogels could immobilize and attach onto the scarfskin, and easily form the designed shape.

Structure and morphology of hydrogels

Figure 4 shows the XRD patterns of the freeze-dried powders of native EPE/CD hydrogel and hybrid EPE/CD/CNT hydrogel as well as α -CD. The XRD patterns of the freeze-dried hydrogel powders were distinctly different from that of α -CD. In the XRD patterns of the freeze-dried hydrogel powders, the characteristic peak of the channel-type crystalline based on the α -CD/PEO inclusion complex, located at 2θ of 19.4° , indicated that the aggregation of PRs

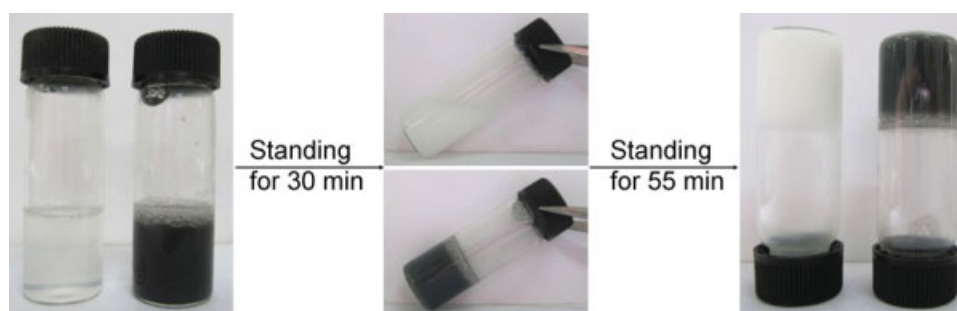


Figure 2 Formation illustration of hybrid EPE/CD/CNT hydrogel as well as native EPE/CD hydrogel.

was still a basic building unit in the native and hybrid hydrogels, and played a key role of physical crosslinking in the formation of hydrogels. In addition, the XRD pattern of the hybrid hydrogel was also slightly different from that of native hydrogel. It might be attributed to the effect of the CNT hybridization on the stacking of PRs.

Moreover, the morphologies of freeze-dried native and hybrid hydrogels were reflected by the SEM images (Fig. 5). As shown in Figure 5(A), the native EPE/CD hydrogel exhibited a loose sponge-like structure, resulting from the leakage of the trapped water during freeze-drying. The hybrid EPE/CD/CNT hydrogel in Figure 5(B) almost inherited this kind of loose structure, but many agglomerates

showed a crystalline character which might be attributed to the nucleation of CNT.

Shear-thinning properties of hydrogels

The steady rheological behaviors of the hybrid EPE/CD/CNT hydrogel and native EPE/CD hydrogel are depicted in Figure 6. The viscosity of the native hydrogel, functioned as an increase of shear rate, gradually diminished. Such shear-thinning property, as the unique character of supramolecular hydrogel, was inherited by the CNT-hybridized hydrogel. As is well known, the formation and stability of this supramolecular hydrogels depended upon the physical crosslinking based on the aggregation of PRs. Meanwhile, the PR was also stabilized by hydrogen bonding among CDs as well as hydrophobic interactions between CD inner and included PEO segment. As a result, the shear-thinning behaviors of native and hybrid hydrogels were mainly attributed to the

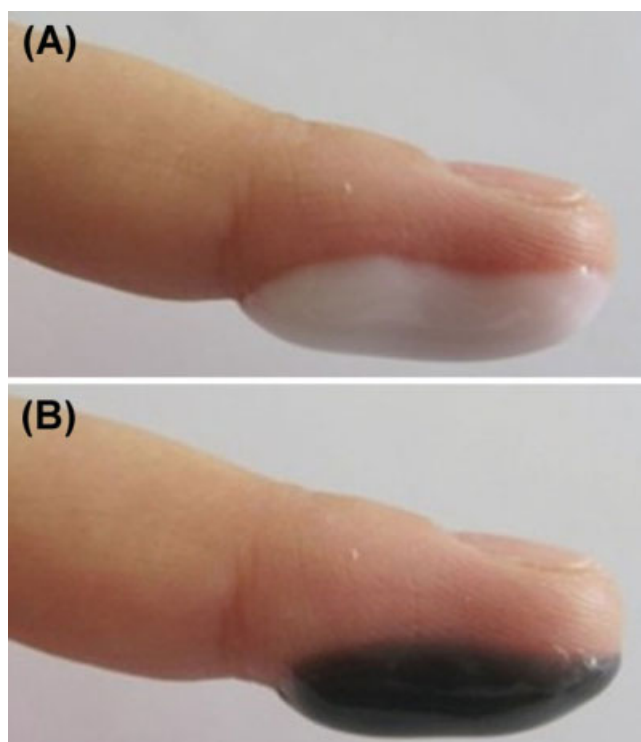


Figure 3 Visualizing adhesions of native EPE/CD hydrogel (A) and its CNT-hybridized hydrogel (B) on the skin of human being. [Color figure can be viewed in the online issue, which is available at www.interscience.wiley.com.]

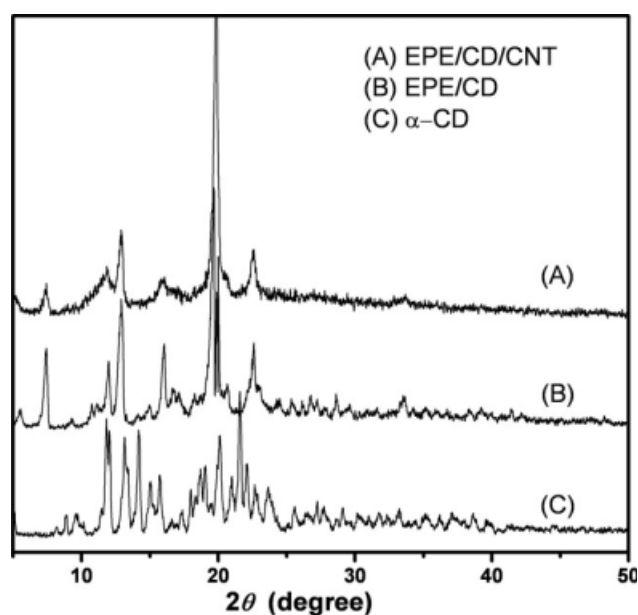


Figure 4 XRD patterns of the freeze-dried hybrid EPE/CD/CNT hydrogel (A) and native EPE/CD hydrogel (B) as well as the reference of pure α -CD (C).

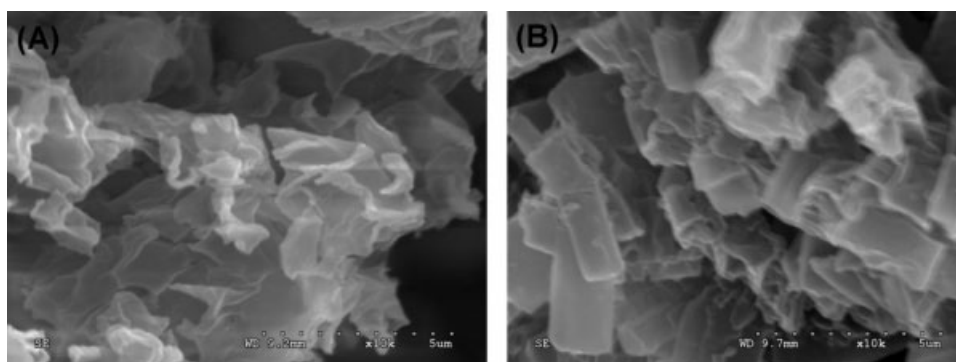


Figure 5 SEM images of freeze-dried native EPE/CD hydrogel (A) and hybrid EPE/CD/CNT hydrogel (B).

cleavage of physical interactions mentioned above, and provided the way to regulate reversible gel-sol transition.

Mechanical reinforcement of CNT

Figure 7 depicts the dynamic rheological behaviors of native and hybrid hydrogels. The storage modulus (G') values of native and hybrid hydrogels exhibited a substantial elastic response, which were greater than the loss modulus (G'') over the entire range of frequency, indicating the formation of strong and rigid hydrogels. Different from the previous report on the decline of G' due to the incorporation of SWCNT,²⁰ the storage modulus (G') of the CNT-hybridized hydrogel was slightly higher than that of native hydrogel after decreasing the molar ratio of CD vs. EO designedly. Although the interaction between CNT and PPO segments inhibited the aggregation of PPO segments as the other physical crosslinking of driving gelation,¹⁵ the CNT enhanced the G' values by virtue of mechanical reinforcement

of its distinct nanostructure with relatively higher stiffness. Meanwhile, the hydrophobic interaction between CNT and PPO segment provided the essential associations for mechanical reinforcement. In addition, it must be mentioned that the G'' value of hybrid hydrogel was lower than that of native hydrogel. It indicated that the hybrid hydrogel exhibited higher damping capacity.

Water-retention performance of hydrogels

A good adhesion onto scarfskin contributed to the application of these hydrogels as wound dressing. As a result, low water-loss of hydrogels was required. Figure 8 shows the water-loss functioned as the time for the native and hybrid hydrogels. During the initial 3 h, the water loss of two hydrogels was less than 10% due to slow volatilization of superficial water. However, with the prolongation of time, the inner water gradually diffused onto the surface and then evaporated, resulting in a gradual increase of water loss for both the native and hybrid

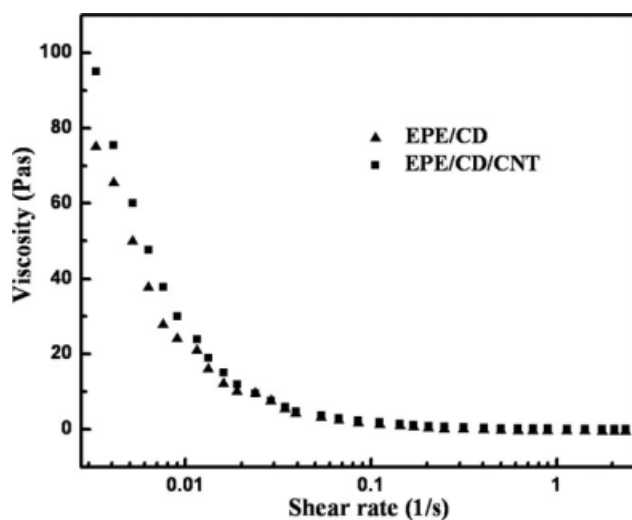


Figure 6 Steady rheological behaviors of native EPE/CD hydrogel and hybrid EPE/CD/CNT hydrogel.

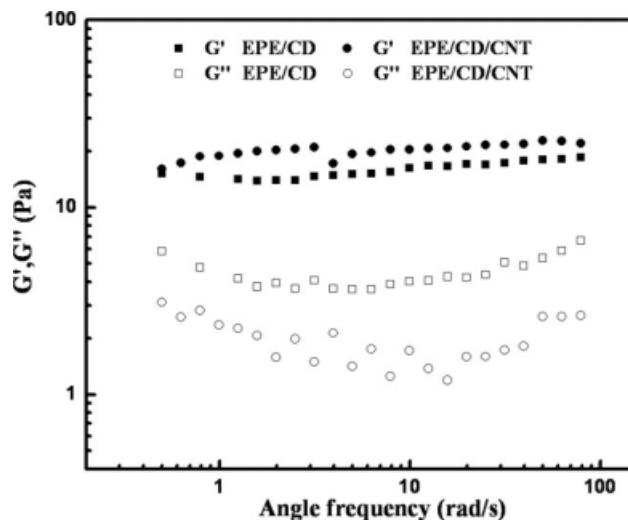


Figure 7 Dynamic rheological behaviors of native EPE/CD hydrogel and hybrid EPE/CD/CNT hydrogel.

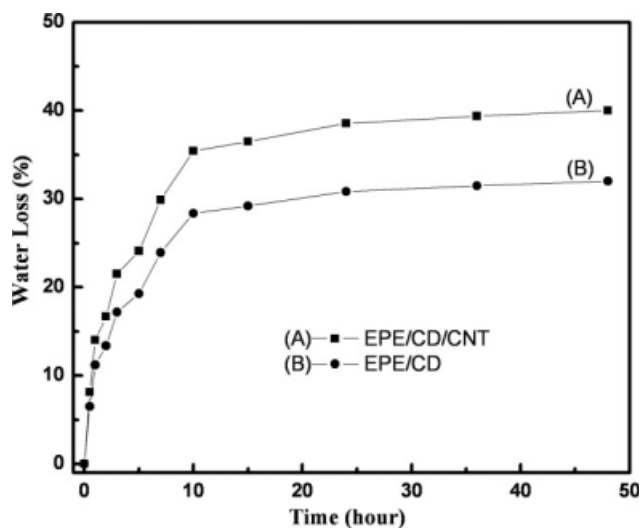


Figure 8 Dependence of water-loss on the time for hybrid EPE/CD/CNT hydrogel (A) and native EPE/CD hydrogel (B).

hydrogels. After 10 h, the weight loss of the native and hybrid hydrogels was kept as 30 and 40%, respectively. The higher water loss of hybrid hydrogel resulted from the hydrophobicity of incorporated CNTs. On the whole, it could be clearly seen that both the native and hybrid hydrogel exhibited low water loss. It was attributed to the absorption of hydrophilic components to water molecules as well as the inhibition of internal network to the diffusion of water molecules in the hydrogels. As a result, the favorable water-retention performance of hydrogels is propitious to wound healing and drug release as expected.

Antimicrobial activity of hydrogels

Antimicrobial activity is another basis as wound dressing. Table I summarizes the data of BRR and the diameters of inhibition zone for the hybrid and native hydrogels against *Escherichia coli* and

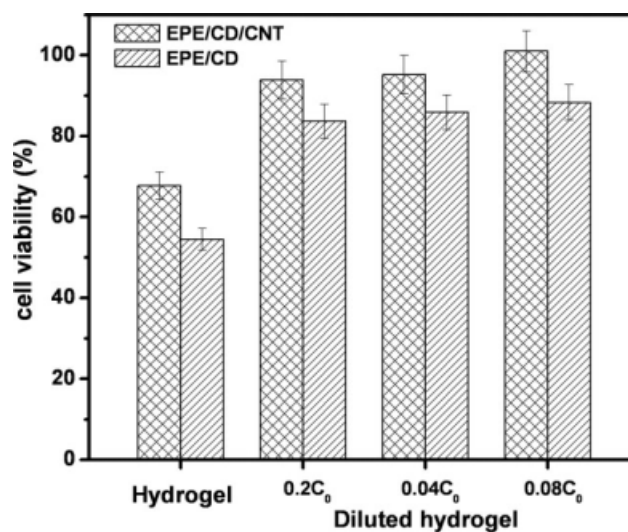


Figure 9 Cytotoxicity of native EPE/CD hydrogel and hybrid EPE/CD/CNT hydrogel at different concentrations for 24 h.

Staphylococcus aureus, respectively. It could be seen that the BRR value of the EPE/CD/CNT hydrogels was higher than the native EPE/CD hydrogel, indicating that the EPE/CD/CNT hydrogel had a better antimicrobial activity than the native EPE/CD hydrogel. Meanwhile, both hydrogels also showed the antibacterial effect against *Escherichia coli* higher than *Staphylococcus aureus*.

Cytotoxicity of hybrid and native hydrogels

As a potential injectable biomaterial, the cytotoxicity of CNT-hybridized hydrogel is a key issue. Cell viability assay was performed to evaluate the *in vitro* cytotoxicity of the hydrogels with and without the introduction of CNT. As illustrated in Figure 9, the cell viability of EPE/CD was above 60% even after 24 h of incubation at a hydrogel dose of 10 $\mu\text{g mL}^{-1}$. At the same time, the EPE/CD/CNT hybrid hydrogel showed comparative cytotoxicity with that of

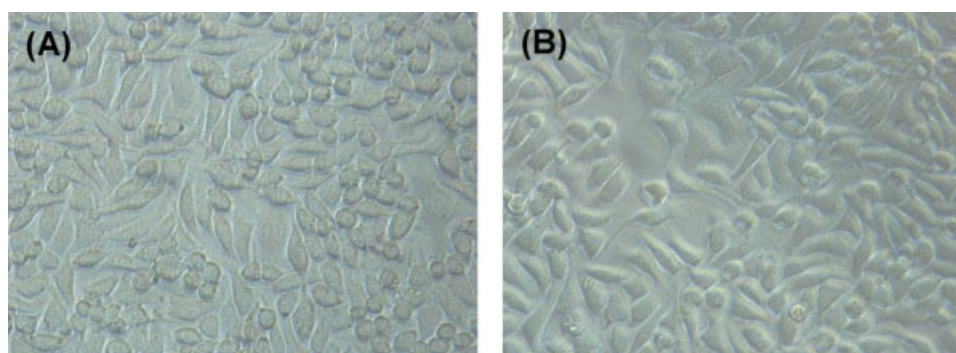


Figure 10 Phase-contrast photomicrographs of L-929 cells with native EPE/CD hydrogel (A) and hybrid EPE/CD/CNT hydrogel (B) for 24 h. [Color figure can be viewed in the online issue, which is available at www.interscience.wiley.com.]

EPE/CD hydrogel at the same dosage. It suggested that the introduction of CNT still kept the relatively low cytotoxicity of EPE/CD hydrogels. The cytotoxicity of EPE/CD and EPE/CD/CNT hybrid hydrogels was also verified by observing of L-929 cell growth condition. Figure 10(A,B) showed the phase-contrast photomicrographs of L-929 cell treated with EPE/CD and EPE/CD/CNT hydrogel ($10 \mu\text{g mL}^{-1}$) for 24 h. The good cell growth conditions further confirmed their low cytotoxicity.

CONCLUSIONS

In this work, the properties of CNT-hybridized supramolecular EPE/CD hydrogels, as an injectable biomaterial and wound dressing, were investigated. The antimicrobial activity, skin-adhesion, and water-retention performances of hybrid supramolecular hydrogel were verified to meet the need as a wound dressing. Meanwhile, the cell viability assay verified the cytotoxicity of the hybrid hydrogels, which was equivalent to the native EPE/CD hydrogels. After the network density of hydrogel was designedly decreased to improve the diffusion of encapsulated substances, the CNT played a role of mechanical reinforcement, and resulted in the increase of storage modulus. In addition, the incorporation of CNT could decrease the gelation time, and the CNT-hybridized hydrogel still kept the shear-thinning property. These were suitable to the methodology of injectable implantation. In conclusion, the CNT-hybridized supramolecular hydrogels showed a great potential in the biomedical application.

References

- Ciferri, A. *Supramolecular Polymers*; Marcel Dekker: New York, 2000.
- Wenz, G.; Han, B. H.; Müller, A. *Chem Rev* 2006, 106, 782.
- Huang, F.; Gibson, H. W. *Prog Polym Sci* 2005, 30, 982.
- Choi, H. S.; Yamamoto, K.; Ooya, T.; Yui, N. *ChemPhysChem* 2005, 6, 1081.
- Choi, H. S.; Kontani, K.; Huh, K. M.; Sasaki, S.; Ooya, T.; Lee, W. K.; Yui, N. *Macromol Biosci* 2002, 2, 298.
- He, L.; Huang, J.; Chen, Y.; Xu, X.; Liu, L. *Macromolecules* 2005, 38, 3845.
- Zhao, S. P.; Zhang, L. M.; Ma, D.; Yang, C.; Yan, L. *J Phys Chem B* 2006, 110, 12225.
- Zhao, S. P.; Zhang, L. M.; Ma, D. *J Phys Chem B* 2006, 110, 16503.
- Li, J.; Loh, X. J. *Adv Drug Deliv Rev* 2008, 60, 1000.
- Li, J.; Ni, X.; Leong, K. W. *J Biomed Mater Res* 2003, 65, 196.
- Yuan, R. X.; Shuai, X. T. *J Polym Sci Part B: Polym Phys* 2008, 46, 782.
- Wu, D.; Wang, T.; Lu, B.; Cheng, S. X.; Jiang, X. J.; Zhang, X. Z.; Zhuo, R. X. *Langmuir* 2008, 24, 10306.
- Li, J.; Li, X.; Ni, X.; Wang, X.; Li, H.; Leong, K. W. *Biomaterials* 2006, 27, 4132.
- Li, X.; Li, J. *J Biomed Mater Res A* 2008, 86, 1055.
- Li, J.; Li, X.; Zhou, Z.; Ni, X. P.; Leong, K. W. *Macromolecules* 2001, 34, 7236.
- Manakker, F.; Pot, M.; Vermonden, T.; Nostrum, C. F.; Hennink, W. E. *Macromolecules* 2008, 41, 1766.
- Wei, H.; Zhang, A.; Qian, L.; Yu, H. Q.; Hou, D. D.; Qiu, R. X.; Feng, Z. G. *J Polym Sci Part A: Polym Chem* 2005, 43, 2941.
- Sabadini, E.; Cosgrove, T. *Langmuir* 2003, 19, 9680.
- Zhou, X.; Chen, L.; Yan, D. *Langmuir* 2004, 20, 484.
- Wang, Z.; Chen, Y. *Macromolecules* 2007, 40, 3402.
- Ma, D.; Zhang, L. *J Phys Chem B* 2008, 112, 6315.
- Guo, M.; Jiang, M.; Pispas, S.; Zhou, C. X.; Yu, W. *Macromolecules* 2008, 41, 9744.
- Lu, F.; Gu, L.; Meziani, M. J.; Wang, X.; Luo, P. G.; Veca, L. M.; Cao, L.; Sun, Y.-P. *Adv Mater* 2009, 21, 139.
- Veetil, J. V.; Ye, K. *Biotechnol Prog* 2007, 23, 517.
- Liu, Z.; Sun, X.; Nakayama, R. N.; Dai, H. *ACS Nano* 2007, 1, 50.
- Dhar, S.; Liu, Z.; Thomale, J.; Dai, H.; Lippard, S. J. *J Am Chem Soc* 2008, 130, 11467.
- Kam, N. W. S.; O'Connell, M.; Wisdom, J. A.; Dai, H. *Proc Natl Acad Sci USA* 2005, 102, 11600.
- Porter, A. E.; Gass, M.; Muller, K.; Skepper, J. N.; Midgley, P. A.; Welland, M. *Nat Nanotechnol* 2007, 2, 713.
- Harrison, B. S.; Atala, A. *Biomaterials* 2007, 28, 344.
- Abarrategi, A.; Gutiérrez, M. C.; Moreno, V. C.; Hortiguera, M. J.; Ramos, V.; LopezLacomba, J. L.; Ferrer, M. L.; Monte, F. *Biomaterials* 2008, 29, 94.
- Usui, Y.; Aoki, K.; Narita, N.; Murakami, N.; Nakamura, I.; Nakamura, K.; Ishigaki, N.; Yamazaki, H.; Horiuchi, H. *Small* 2008, 4, 240.
- Macdonald, R. A.; Voge, C. M.; Kariolis, M.; Stegemann, J. P. *Acta Biomater* 2008, 4, 1583.
- Meng, J.; Kong, H.; Han, Z.; Wang, C.; Zhu, G.; Xie, S.; Xu, H. *J Biomed Mater Res A* 2009, 88, 105.
- Fraczek, A.; Menaszek, E.; Paluszkiwicz, C.; Blazewicz, M. *Acta Biomater* 2008, 4, 1593.
- Zhang, D.; Kandadai, M. A.; Cech, J.; Roth, S.; Curran, S. A. *J Phys Chem B* 2006, 110, 12910.
- Moore, V. C.; Strano, M. S.; Haroz, E. H.; Schmidt, J.; Talmon, Y.; Hauge, R. H.; Smalley, R. E. *Nano Lett* 2003, 3, 1379.
- Shvartzman, C. R.; Levi, K. Y.; Nativ, R. E.; Yerushalmi, R. R. *Langmuir* 2004, 20, 6085.
- Kurkurim, D.; Kulkarnia, R.; Aminabhavit, M. *Polym Plast Technol Eng* 2002, 41, 469.
- Kurkuri, M. D.; Aminabhavi, T. M. *J Control Release* 2004, 96, 9.